INL/EXT-15-37382

Light Water Reactor Sustainability Program

Application of Nonlinear Seismic Soil-Structure Interaction Analysis for Identification of Seismic Margins at Nuclear Power Plants

Amit H. Varma, Jungil Seo, and Justin Coleman

November 2015

DOE Office of Nuclear Energy

INL/EXT-15-37382

Light Water Reactor Sustainability Program

Application of Nonlinear Seismic Soil-Structure Interaction Analysis for Identification of Seismic Margins at Nuclear Power Plants

Amit H. Varma – Stanex, LLC
Jungil Seo – Stanex, LLC
Justin Coleman – INL

November 2015

Idaho National Laboratory
Idaho Falls, Idaho 83415

http://www.inl.gov/lwrs

Prepared for the
U.S. Department of Energy
Office of Nuclear Energy
Under DOE Idaho Operations Office
Contract DE-AC07-05ID14517

Executive Summary

Seismic probabilistic risk assessment (SPRA) methods and approaches at nuclear power plants (NPP) were first developed in the 1970s and aspects of them have matured over time as they were applied and incrementally improved. SPRA provides information on risk and risk insights and allows for some accounting for uncertainty and variability. As a result, SPRA is now used as an important basis for risk-informed decision making for both new and operating NPPs in the US and in an increasing number of countries globally.

SPRAs are intended to provide best estimates of the various combinations of structural and equipment failures that can lead to a seismic induced core damage event. However, in some instances the current SPRA approach contains large uncertainties, and potentially masks other important events (for instance, it was not the seismic motions that caused the Fukushima core melt events, but the tsunami ingress into the facility).

INL has an advanced SPRA research and development (R&D) activity that will identify areas in the calculation process that contain significant uncertainties. One current area of focus is the use of nonlinear soil-structure interaction (NLSSI) analysis methods to accurately capture: 1) nonlinear soil behavior and 2) gapping and sliding between the NPP and soil.

The goal of this study is to compare numerical NLSSI analysis results with recorded earthquake ground motions at Fukushima Daichii (Great Tohuku Earthquake) and evaluate the sources of nonlinearity contributing to the observed reduction in peak acceleration. Comparisons are made using recorded data in the free-field (soil column with no structural influence) and recorded data on the NPP basemat (in-structure response). Results presented in this study should identify areas of focus for future R&D activities with the goal of minimizing uncertainty in SPRA calculations. This is not a validation activity since there are too many sources of uncertainty that a numerical analysis would need to consider (variability in soil material properties, structural material properties, etc.). Rather the report will determine if the NLSSI calculations are following similar trends observed in the recorded data (i.e. reductions in maximum acceleration between the free-field and basemat)

Numerical NLSSI results presented show maximum accelerations between the free field and basemat were reduced the EW and NS directions. The maximum acceleration in the UD direction increased slightly. The largest reduction in maximum accelerations between the modeled free-field and the NPP basemat resulted in nearly 50% reduction. The observation in reduction of numerical maximum accelerations in the EW and NS directions follows the observed trend in the recorded data.

The maximum reductions observed in these NLSSI studies were due to soil nonlinearities, not gapping and sliding (although additional R&D is needed to develop an appropriate approach to model gapping and sliding). This exploratory study highlights the need for additional R&D on developing: (i) improved modeling of soil nonlinearities (soil constitutive models that appropriately capture cyclic soil behavior), (ii) improved modeling of gapping and sliding at the soil-structure interface (to appropriately capture the dissipation of energy at this interface), and (iii) experimental laboratory test data to calibrate the items (i) and (ii).

CONTENTS

FIGURES

TABLES

Nonlinear Seismic Soil Structure Modeling

1. SUMMARY

Soil-structure interaction (SSI) plays an important role in seismic response of nuclear power plant structures. SSI can have a significant influence on the calculated the in-structure response spectra (ISRS), and the calculated seismic design demand forces for nuclear power plant structures subjected to earthquake loading combinations. Our hypothesis is that nonlinearities in the SSI have the potential to further reduce the peak acceleration demands due to energy dissipation. The sources of these nonlinearities include: (i) nonlinear soil behavior, (ii) nonlinear structure behavior, and (iii) nonlinearities such as gapping and sliding across the soil-structure interface.

The goal of this exploratory study is to compare numerical NLSSI analysis results with measured ground motions, to evaluate sources of nonlinearity contributing to the observed reduction in peak acceleration between the ground and inside the structure. To achieve the goal, a series of linear (SSI) and nonlinear (NLSSI) analyses were performed using ground motion data and site soil profile measured near Fukushima Daichii nuclear power plant Unit 6. The focus of the analyses was on evaluating two specific nonlinear effects from localized soil nonlinearity and gapping and sliding. Other NLSSI effects were not considered in this study for simplicity. Four different SSI models (with variations in nonlinearity) were developed using LS-DYNA, a commercially available finite element analysis software. The seismic responses at three different locations of interest (free field soil, reactor building basemat, and turbine building basemat) from the four different SSI models were compared and evaluated. The following sections present details of the development of the four analysis models and analysis results.

2. FUKUSHIMA DAICHII NUCLEAR POWER PLANT

2.1 Nuclear Power Plant Structure

Fukushima Daichii Unit 6 was considered in this study. It is a boiling water reactor (BWR Mark II) located in the Futaba District of Fukushima Prefecture, Japan. A schematic cross-section view of a typical BWR Mark II containment is shown in Figure 1. As shown, the containment consists of a drywell with the reactor vessel and a wetwell with a pressure suppression pool. In the development of numerical model, the dimensions of Unit 6 (including reactor and turbine buildings) were determined based on a drawing for Fukushima Daichii Units 6 (shown in Figure 1) and site layout of Fukushima Daichii nuclear power plant as shown in Figure 2.

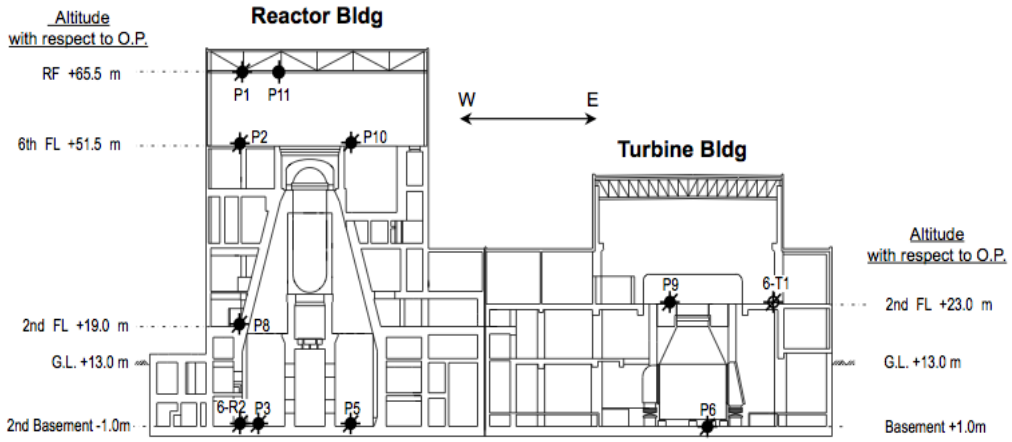

Figure 1. Schematic cross-section view of BWR Mark II containment (Coleman, 2015).

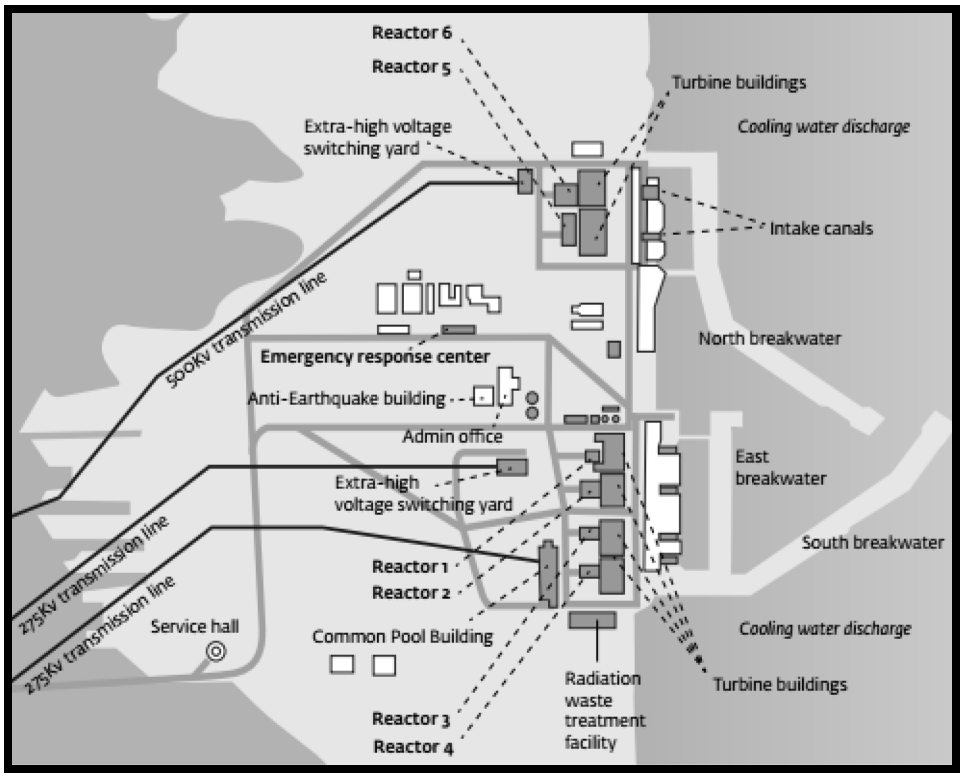

Figure 2. Site layout of Fukushima Daichii nuclear power plant (Coleman, 2015).

2.2 Site Soil Profile

Site details including the location of the observations sites and site soil profiles reported by Coleman (2015) are shown in Figure 3. The soil in Fukushima Daichii Unit 6 is dominantly classified as variations of mudstone. The soil layers present at the site are depicted from the borehole information provided by TEPCO. Table 1 summarizes the provided data from the seismometers located near Unit 6. The maximum recorded acceleration in north-south, east west, and up-down directions, shear wave, and compression wave velocities are listed respectively in gals (cm/s2) and m/s. The elastic soil properties were determined by referencing the Central Federal Lands Highway geophysical methodology and reported by Coleman (2015). The reported elastic soil properties of the site near Unit 6 are summarized in Table 2.

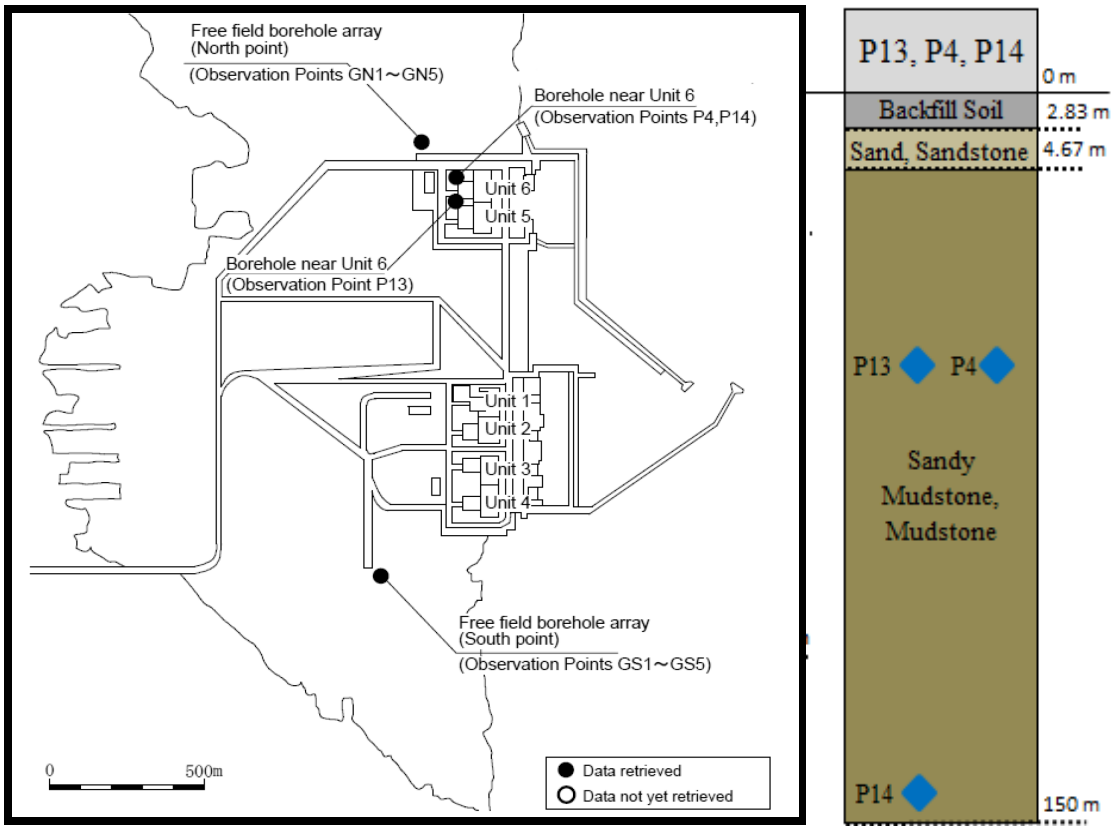

Figure 3. Fukushima Daiichi nuclear power plant schematic locations of boreholes on site and interpreted soil layering near Unit 6 (Coleman, 2015)

Table 1. Maximum Accelerations recorded in three directions for borehole location near Unit 6 (Coleman, 2015).

Location	Depth (m)	Obs. Pt.	Max Acceleration (Gal)			Shear Velocity (m/s)	Compressional Wave (m/s)
			NS	EW	UD		
Borehole near Unit 6	-31.5	P13	252	405	194	470	1710
	-31.5	P4	209	387	189	470	1710
	-143.5	P14	313	302	113	580	1820

Table 2. Elastic soil properties for observation point near Unit 6 (Coleman, 2015).

Location	Obs. Pt.	Density (kg/m^3)	PR	Young's Mod (Pa)	Shear Mod (MPa)
Borehole near Unit 6	P13	252	0.46	1285090459	440.36
	P4	209	0.46	1285090459	440.36
	P14	313	0.44	1966421665	681.14

2.3 Reduction in Maximum Recorded Acceleration

A reduction in the recorded maximum acceleration between the free-field motion and basemat motion was observed and reported by Coleman (2015). Table 3 summarizes the reduction at Unit 6. As presented in the table, the maximum recorded acceleration was reduced by 49.1 % in the NS-direction, 39.3 % in the EW-direction, and 31.8 % in the UD-direction. The reduction in maximum-recorded acceleration led to the hypothesis that relative motion (gapping and sliding) between the soil and basemat may be dissipating energy.

Table 3. Reduction in maximum recorded acceleration at Unit 6 (Coleman, 2015).

Location	Point Id	Location Vertically	Max acceleration (g)		
			EW	NS	UD
Unit 6	P3	1m	0.439	0.296	0.166
Free Field (North Points by Unit 6)	GN1	-2 m	0.713	0.581	0.244

3. NUMERICAL MODELING AND ANALYSIS

3.1 Modeling Approach

3.1.1 Structure

The nonlinear soil structure interaction analysis was performed using the direct method. In the method, the whole system (including structure and soil) is analyzed in a single step which enables simulation with the use of nonlinear material models for the soil and structure, and contact models that simulate separation and sliding at the foundation-soil interface. 3D finite element models were developed to perform the analysis using LS-DYNA, a commercially available finite-element solver.

Figure 4 shows a sample finite element model for Fukushima Daichii Unit 6. About 2,417 solid elements were used for the structure. The dimension and geometry of the unit were approximated based on Figure 2. Note that the structure was simplified by neglecting internal equipment and the reactor core. Additional concrete finite elements were included in the structure to take into account the mass of the reactor unit.

132,934 Beam elements were embedded into the structure to represent reinforcing steel. The steel reinforcement ratio of 2% was assumed for both wall slab. Based on the ratio, the size and spacing of the elements were determined. Acceleration data at the bottom surface of the structure was obtained. Acceleration data of Node 648087 was used for the reactor building and Acceleration data of Node 648824 was used for the turbine building.

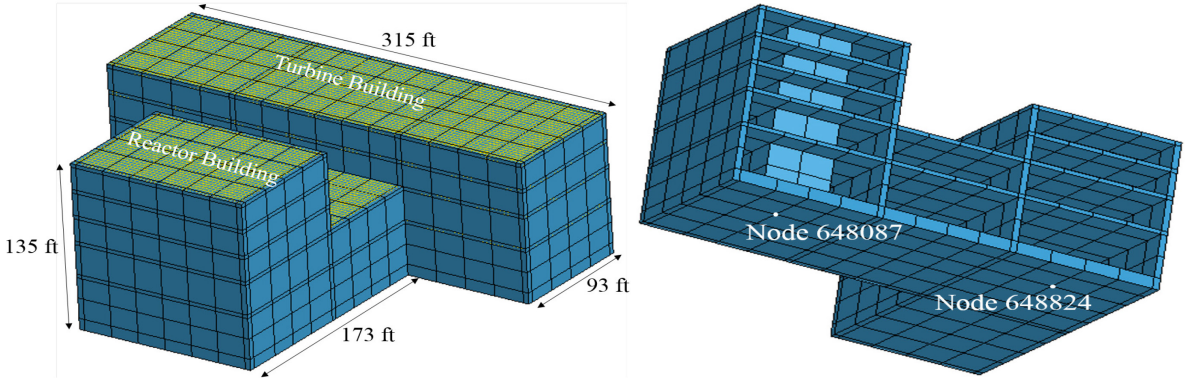

Figure 4. Finite element model for Fukushima Daichii Unit 6.

3.1.2 Soil Domain and Boundary Condition

Figure 5 shows the finite element soil domain with Unit 6 finite element structure model. As shown, the soil domain of the FE model is 2,000 ft x 2,000 ft in plan (more than 6 times the size of the structure (finite element model for Unit 6), and 490 ft deep. The dimensions of the soil domain were determined to be larger than the structure to simulate an infinite domain. The soil domain was built with 297,055 solid elements that have an almost uniform size of 20 ft in all directions.

The base of the soil domain was modeled as a transmitting boundary using the *BOUNDARY_NON_REFLECTING option in LS-DYNA. The ground motion input was applied at the bottom of the soil domain as shown in Figure 6. The boundary nodes at each elevation of the soil domain were constrained to move together in each direction as shown in Figure 7. This enables the elements at the boundaries to move in pure shear, thus simulating a free-field condition.

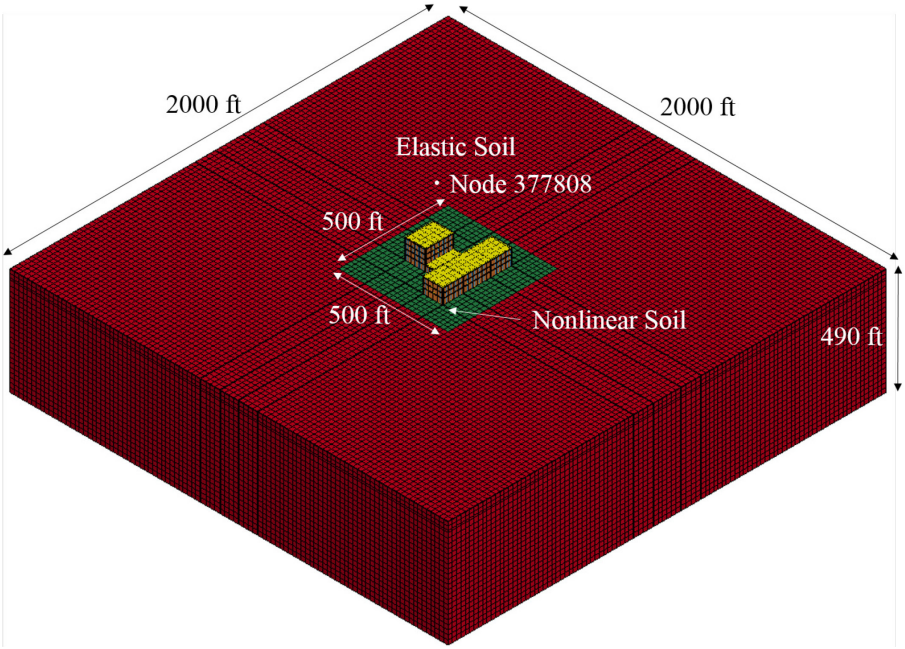

Figure 5. Finite element soil domain with Unit 6 finite element model.

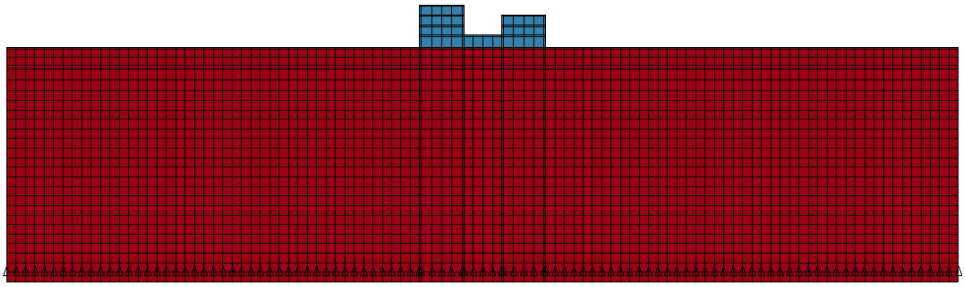

Figure 6. Node set for ground motion input.

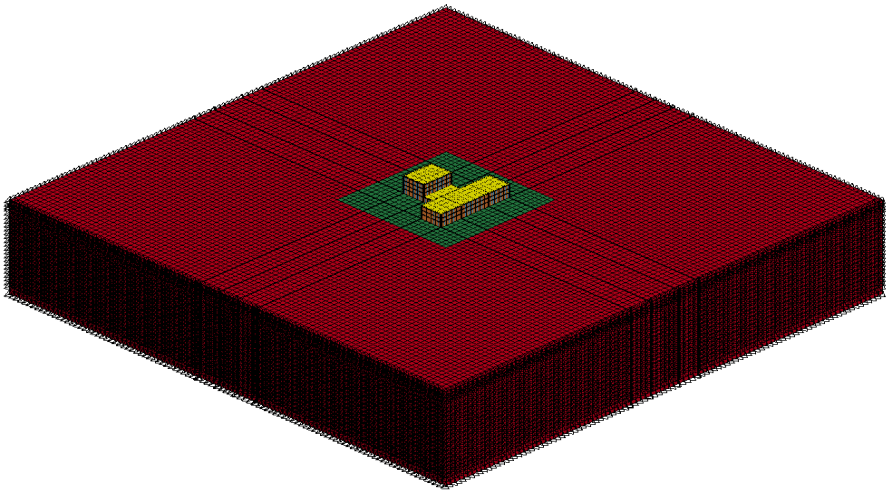

Figure 7. Constrained boundary nodes.

3.1.3 Ground Motion Data

The ground motion data measured from an observation point (P14) located near Unit 6 was used as the ground motion input for the FE model. The acceleration time histories in three directions (NS, EW, and UD) are shown in Figure 8. The maximum acceleration at each direction is summarized in Table 4. Only the section with the maximum intensity (shaded area in Figure 8) was selected and to input into the FE model in each direction.

Table 4. Summary of ground motion input.

Location	Location Vertically	Max acceleration (Gal)		
		NS	EW	UD
P14	-130 m	0.758	0.831	0.288

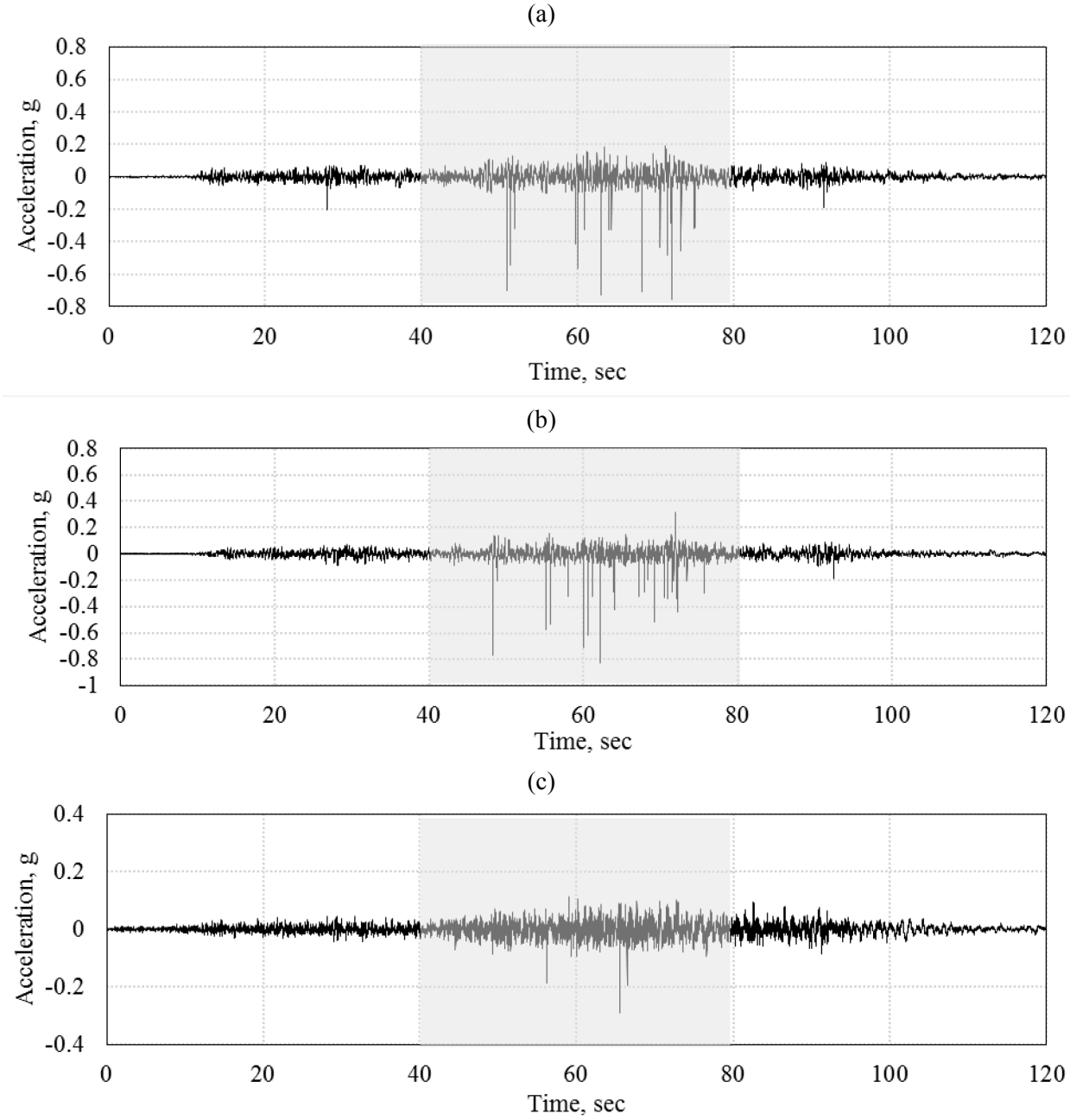

Figure 8. Ground motion data: (a) EW direction, (b) NS direction, and (c) UD direction.

3.2 Linear Analysis

A linear soil-structure interaction (LSSI) analysis with no source of material or geometric nonlinearities was performed to compare the results from the LSSI to those from NLSSI analysis. The same soil domain, structure model, and boundary and loading conditions were used in the analysis. The reported soil material properties (including elastic modulus, poison's ratio, and mass density) were used in the model. Nodes shared by two adjacent parts (elastic soil and structure) were merged to move together.

Figure 9 and Table 5 present the summary of the LSSI analysis results. The maximum accelerations at the free field, the bottom of reactor building basemat (RB-BM), and the bottom of turbine building basemat (TB-

BM) are compared in the figure and the table. Figure 10 also shows the time history responses at the three locations in three different directions (EW, NS, and UD). As shown in the figures and the table, maximum acceleration values at RB-BM and TB-BM were reduced by 13.1 % in the EW direction and 27.8 % in the NS direction. However, the value increased by 10.5 % in the UD direction. The time history responses were converted to response spectra using the Fast Fourier Transform theorem. The converted response spectra are shown in Figure 11. The same tendency can be seen from the figure.

Table 5. Summary of LSSI analysis results.

	Maximum Acceleration, g			
Locations	Node Number	EW	NS	UD
Free Field (FF)	377808	0.580	0.457	0.370
Reactor Building Basemat (RB-BM)	648087	0.496	0.319	0.433
Turbine Building Basemat (TB-BM)	648824	0.512	0.341	0.385

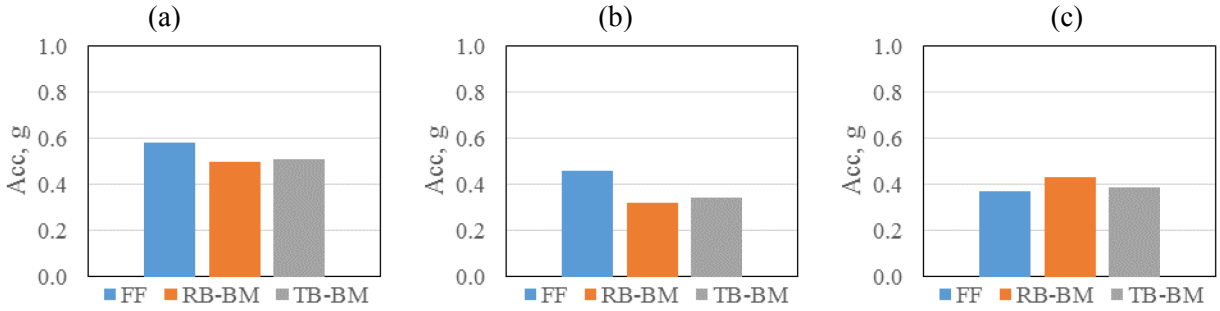

Figure 9. Comparison of maximum acceleration value calculated from LSSI analysis, Free Field (FF), Reactor Basemat (RB-BM), Turbine Basemat (TB-BM): (a) EW direction, (b) NS direction, and (c) UD direction.

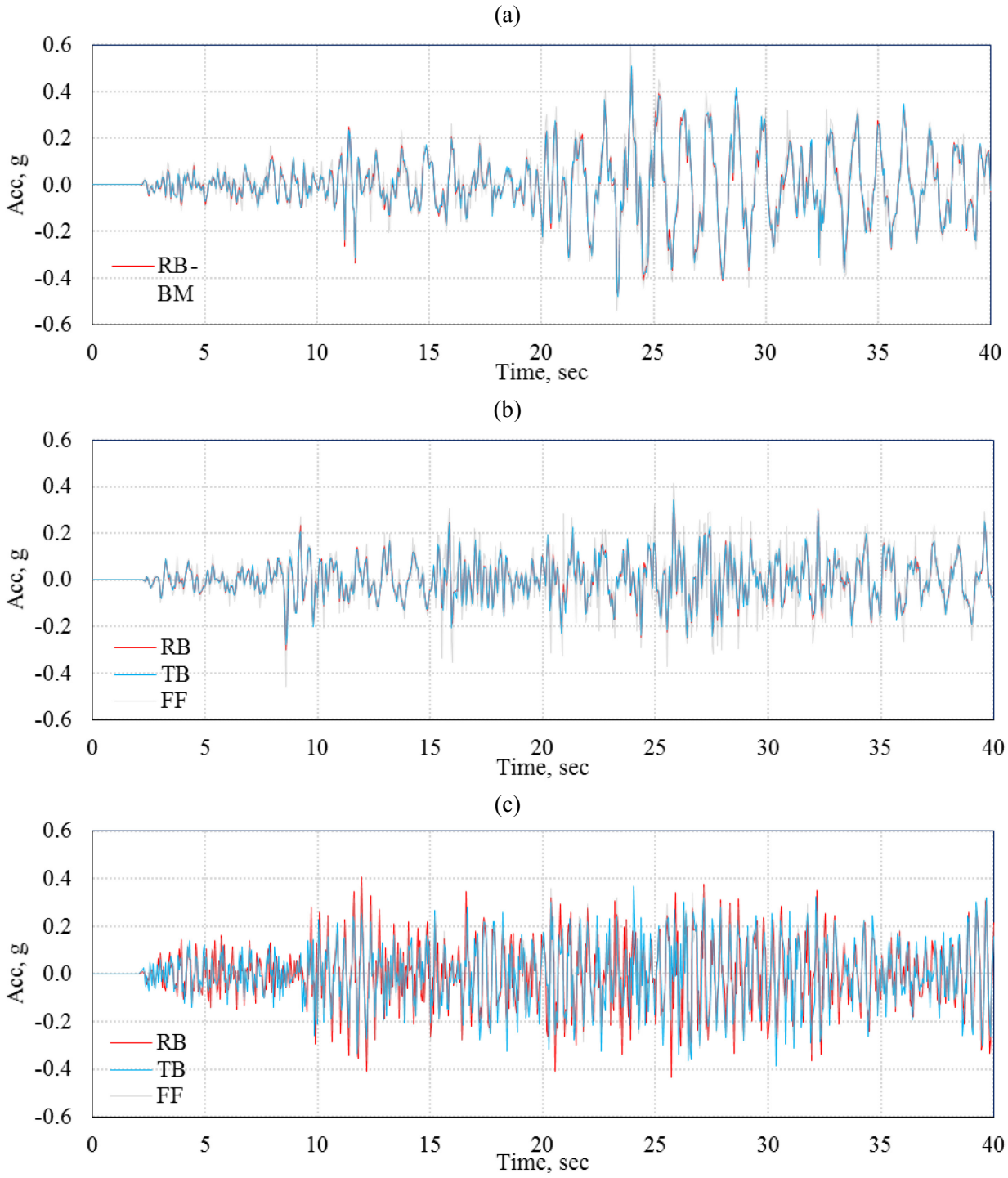

Figure 10. Time history response estimated by LSSI analysis: (a) EW direction, (b) NS direction, and (c) UD direction.

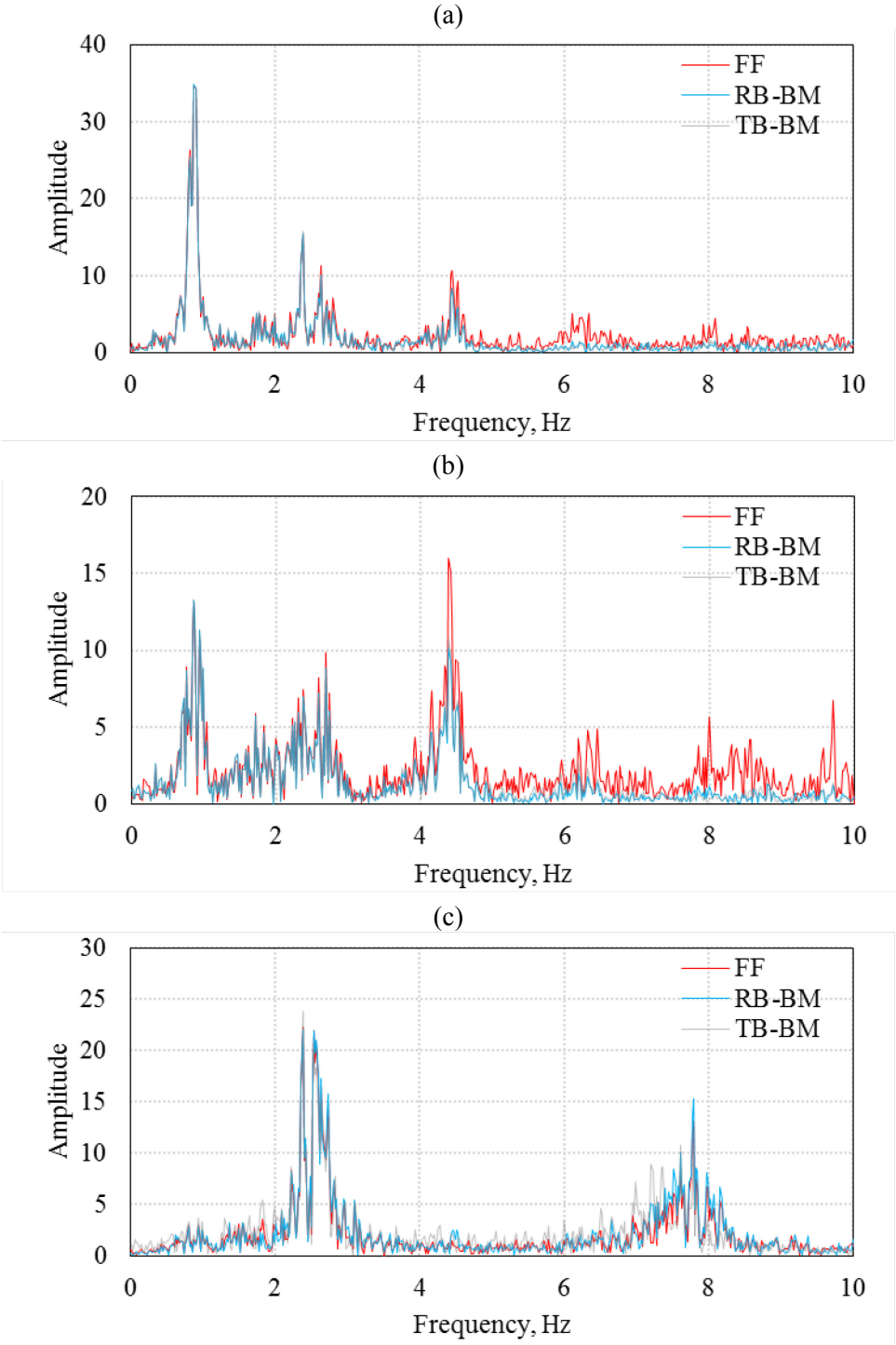

Figure 11. Response spectra on the free field, RB-BM, and TB-BM converted using the Fast Fourier Transform theorem: (a) EW direction, (b) NS direction, and (c) UD direction.

3.3 Nonlinear Analysis

Soil material and geometric nonlinearities (gapping and sliding) were considered in the nonlinear soil-structure interaction (NLSSI) analysis. To evaluate the influence of each source, a series of NLSSI analyses

were performed as summarized in Table 6. The results from NLSSI-S case is used to evaluate the influence of nonlinear soil around the structure on the reduction of the maximum acceleration. NLSSI-TB and NLSSI-G are similar to NLSSI-S with the exception that two different interaction modeling options were considered. For the NLSSI-TB case, tiebreak contact in LS-DYNA was use. For the NLSSI-G case, gap elements were used between the nonlinear soil and the structure.

3.3.1 Ground Motion Data

Figure 12 shows a cross-section view of the NLSSI-S case model. As illustrated in the figure, the structure (Unit 6) is surrounded by nonlinear soil (indicated in green). The shear modulus, mass density and Poisson's ratio used for the linear soil (indicated in red) were also used for the nonlinear soil. The nonlinear soil was modeled using the *MAT_HYSTERETIC material model in LS-DYNA. Figure 13 shows the backbone curve used to model the nonlinear soil. Nodes shared by the linear soil, nonlinear soil, and structure were merged to move together, similar to the linear analysis.

Figure 14 and Table 7 present the summary of the results from the LSSI-S analysis case. The maximum accelerations at the free field, the bottom of reactor building basemat (RB-BM), and the bottom of turbine building basemat (TB-BM) are compared in the figure and the table. Figure 15 also shows the time history responses at the three locations in three different directions (EW, NS, and UD). As shown in the figures and the table, maximum acceleration values at RB-BM and TB-BM were reduced by 29.2 % in the EW direction, 49.8 % in the NS direction, and 21.6 % in the UD direction. The response spectra converted from the time history responses using the Fast Fourier Transform theorem are shown in Figure 16. The same tendency can be seen from the figure.

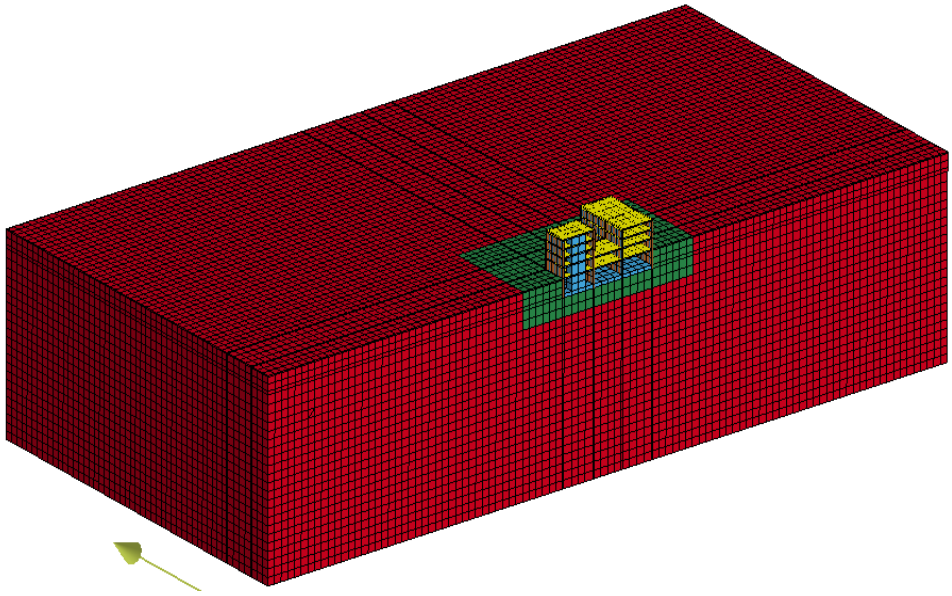

Figure 12. Section view of NLSSI-S case model illustrating the nonlinear soil (green), linear soil (red) and structure (blue).

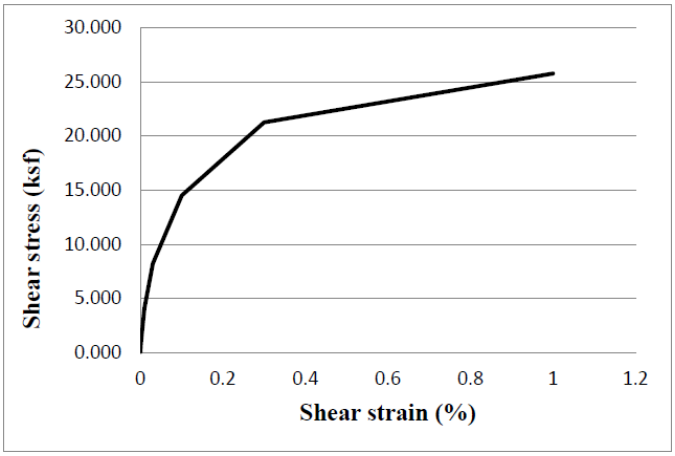

Figure 13. Backbone curve used in the nonlinear soil (Bolisetti and Coleman, 2015).

Table 6. Results of NLSSI-S analysis case.

	Maximum Acceleration, g			
Locations	Node Number	EW	NS	UD
Free Field (FF)	377808	0.602	0.392	0.454
Reactor Building Basemat (RB-BM)	648087	0.421	0.286	0.360
Turbine Building Basemat (TB-BM)	648824	0.432	0.286	0.352

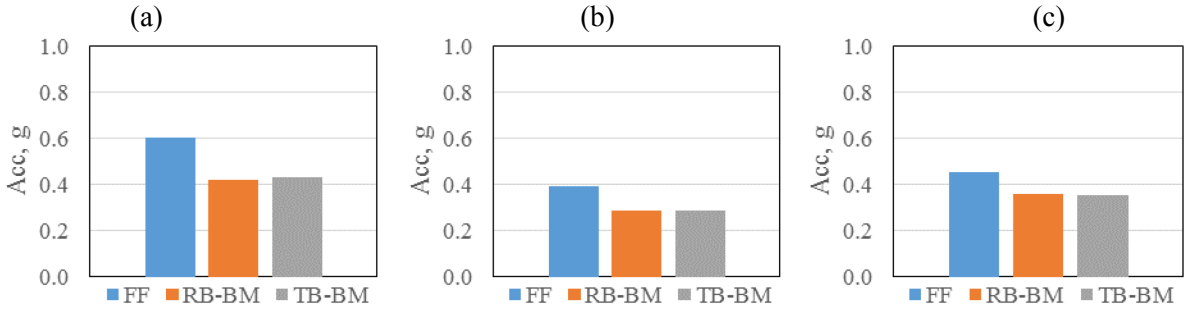

Figure 14. Comparison of maximum acceleration value calculated from LSSI-S analysis case, Free Field (FF), Reactor Basemat (RB-BM), Turbine Basemat (TB-BM): (a) EW direction, (b) NS direction, and (c) UD direction.

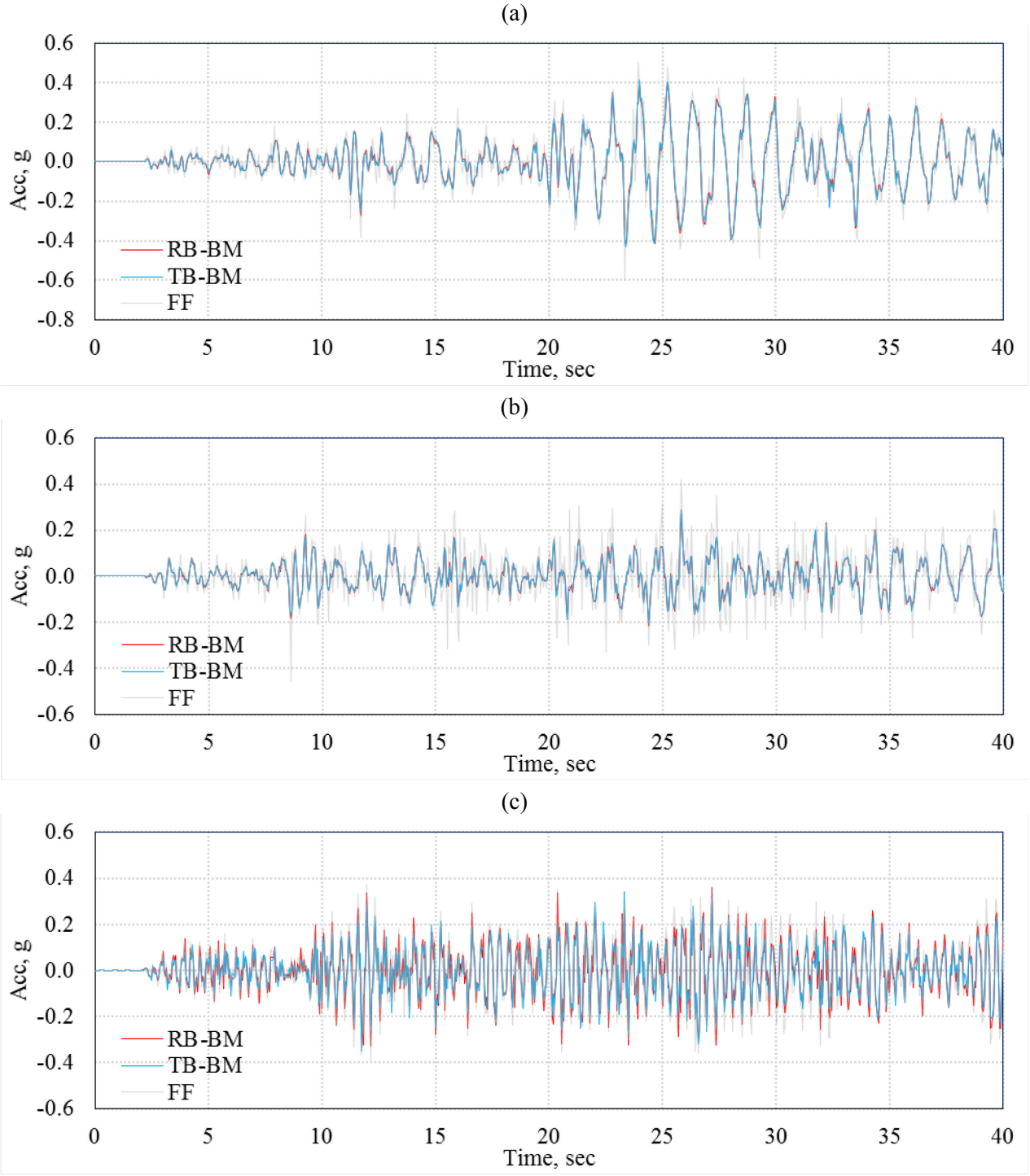

Figure 15. Time history response estimated by LSSI-S analysis case: (a) EW direction, (b) NS direction, and (c) UD direction.

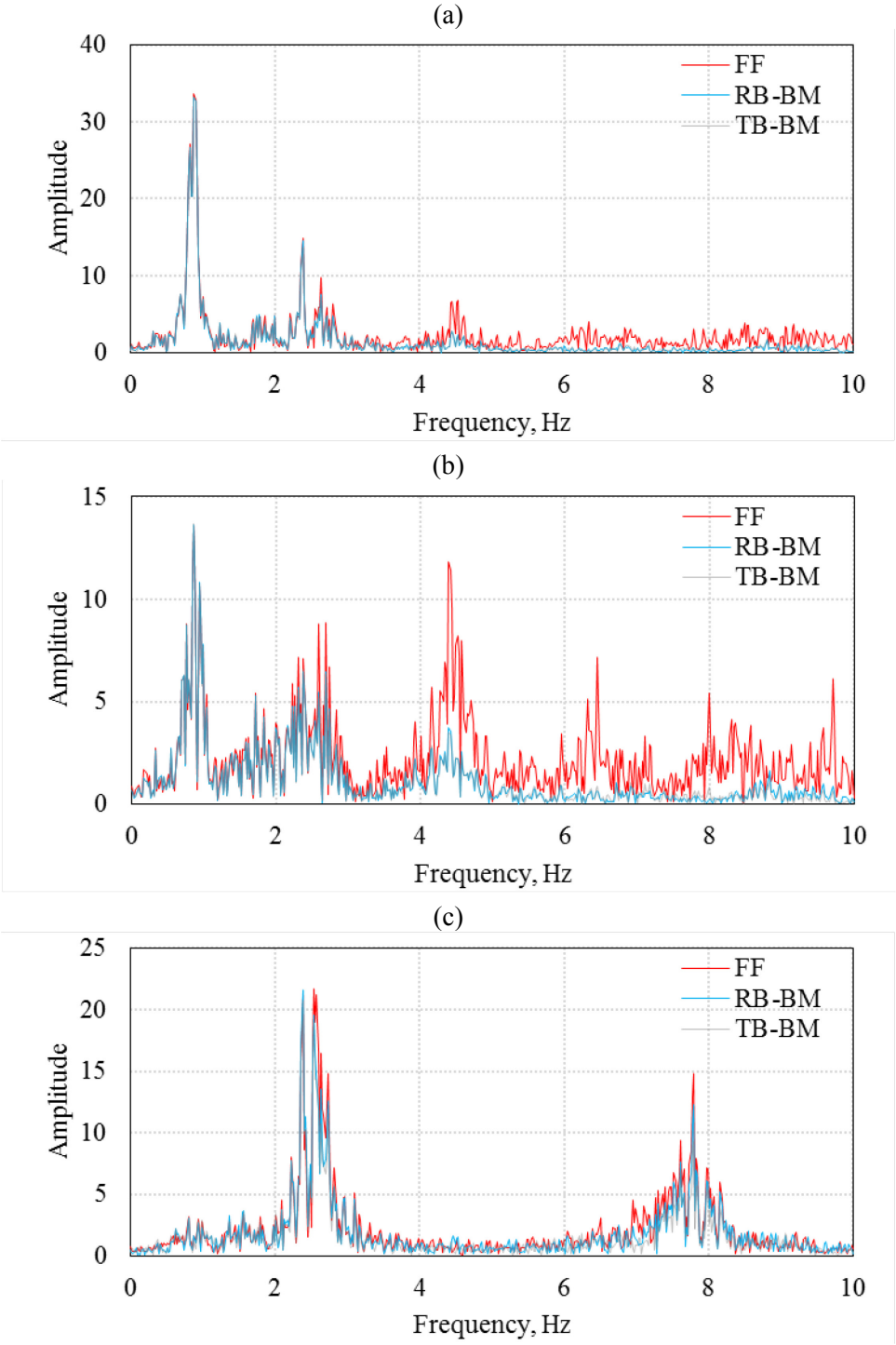

Figure 16. Response spectra on the free field, RB-BM, and TB-BM converted using the Fast Fourier Transform theorem: (a) EW direction, (b) NS direction, and (c) UD direction.

3.3.2 NLSSI-TB

The FE model for the NLSSI-TB is identical to that for NLSSI-S including the nonlinear soil material model, soil material properties, and the structure. However, this analysis cases included a modeling approach to

account for geometric nonlinearities (gapping and sliding). Gapping and sliding between the nonlinear soil and the structure can be idealized as illustrated in Figure 17. It was assumed that gapping occurs when the applied tension demand (force) exceeds the maximum tension capacity of the interaction and sliding occurs when the applied shear demand (force) exceeds the maximum shear capacity of the interaction. For the sake of this exploratory study, it was assumed that the tension capacity of the interaction was equal to the typical tensile strength of soil (0.01 ksf) and the shear capacity of the interaction was equal to the maximum shear strength of the nonlinear soil (22.33 ksf). The *contact_automatic_one_way_surface_to_surface_tiebreak contact in LS-DYNA was defined between the nonlinear soil and the structure with failure criterion of 0.01 ksf for tensile failure stress and 22.33 ksf for shear failure strain.

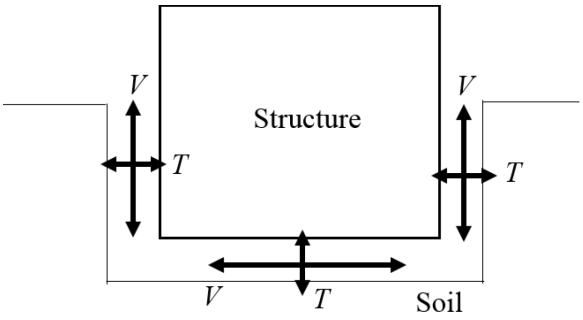

Figure 17. Idealized soil-structure interaction.

Figure 18 and Table 8 present the summary of the results from the LSSI-TB analysis case. The maximum accelerations at the free field, the bottom of reactor building basemat (RB-BM), and the bottom of turbine building basemat (TB-BM) are compared in the figure and the table. Figure 19 also shows the time history responses at the three locations in three different directions (EW, NS, and UD). As shown in the figures and the table, maximum acceleration values at RB-BM and TB-BM were not reduced. Instead, maximum acceleration values at RB-BM and TB-BM increased by up to 173 %. This unrealistic amplifications in the structure are due to the reversion to non-automatic contact after failure.

Table 7. Results of NLSSI-TB analysis case.

	Maximum Acceleration, g			
Locations	Node Number	EW	NS	UD
Free Field (FF)	377808	0.588	0.505	0.400
Reactor Building Basemat (RB-BM)	648087	0.821	0.821	1.094
Turbine Building Basemat (TB-BM)	648824	0.849	0.562	1.003

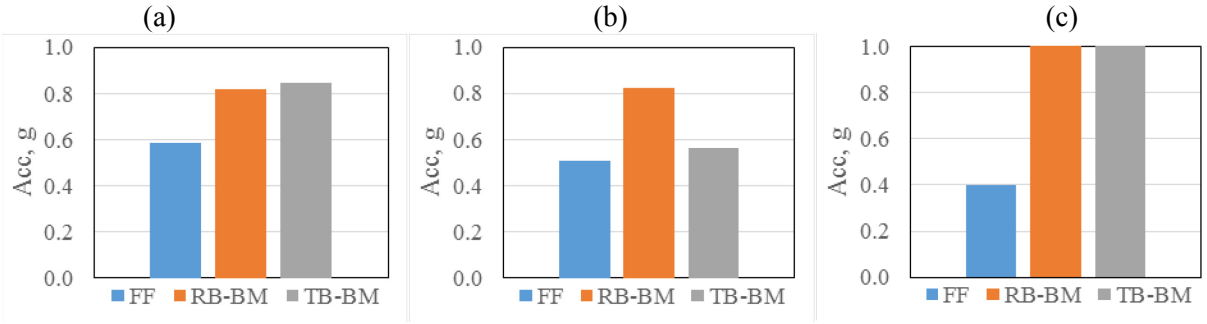

Figure 18. Comparison of maximum acceleration value calculated from LSSI-TB analysis case, Free Field (FF), Reactor Basemat (RB-BM), Turbine Basemat (TB-BM): (a) EW direction, (b) NS direction, and (c) UD direction.

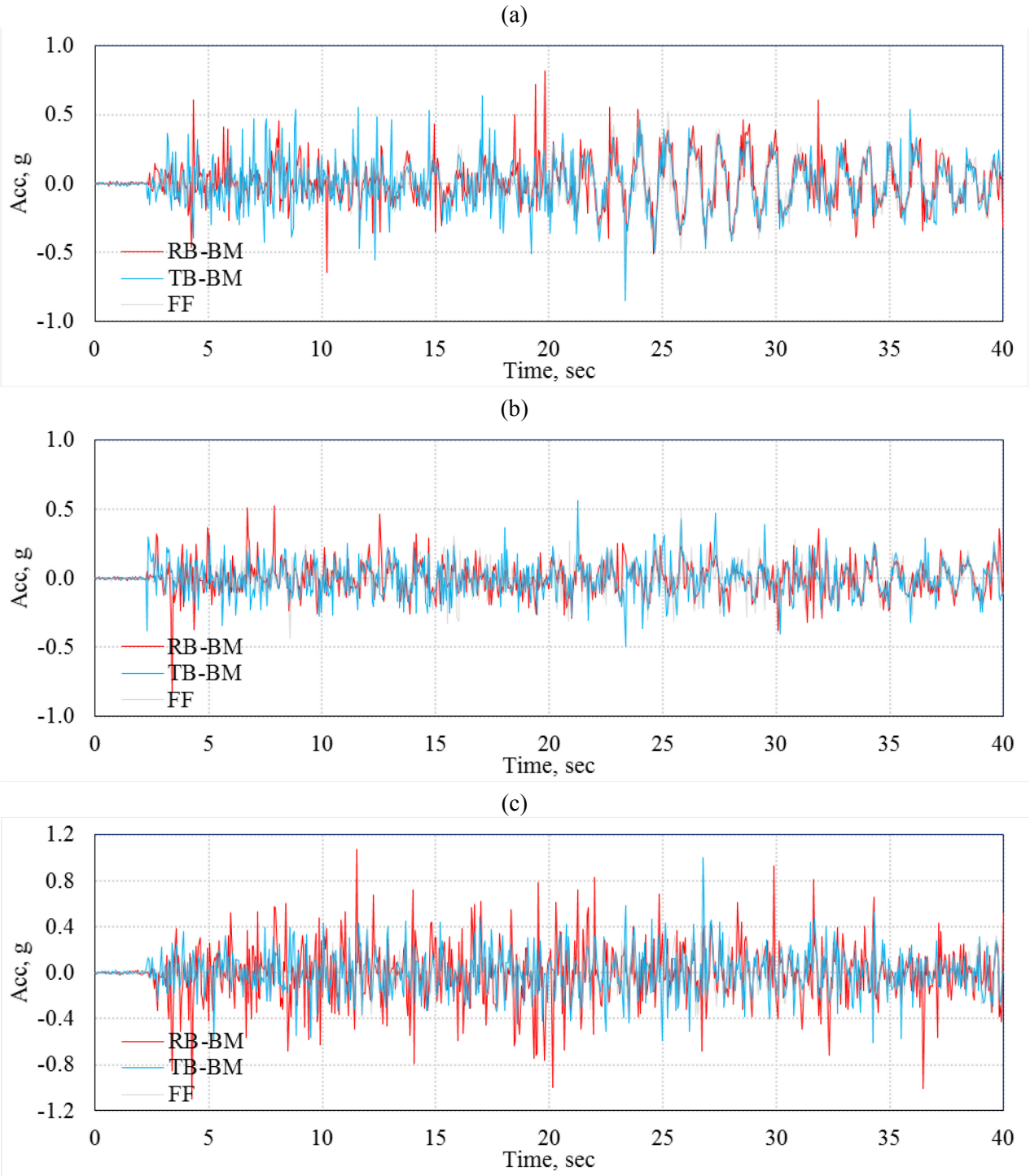

Figure 19. Time history response estimated by LSSI-TB analysis case: (a) EW direction, (b) NS direction, and (c) UD direction.

3.3.3 NLSSI-G

The FE model for the NLSSI-G is the same as the NLSSI-TB analysis model. However, the contact interaction of the NLSSI-TB model was replaced with gap elements to simulate the geometric nonlinearity (gapping and sliding) effects as shown in Figure 20. The *MAT_BRITTLE_DAMAGE material model in LS-

DYNA was used for the gap elements. The elastic soil properties were used for the material model and the same failure criterion as discussed in Section 3.3.2 were assigned to the material model. However, the post-failure behavior (tension and shear) of the gap elements were assumed. The objective was to remove the unrealistic acceleration amplification due to the reversion to non-automatic contact after failure. Therefore, fracture toughness and shear retention factor were additionally assigned to the model.

Reasonable values for the fracture toughness and shear retention factor are recommended in LS-DYNA manual (LSTC, 2013) for a standard grade concrete (E_c = 3.15x10^6 psi, f_t =450 psi, and f_s = 2100) based on a variety of experimental data. Since the gap elements are made of soil material rather than concrete, the recommended values for the fracture toughness and shear retention factor were scaled down based on typical soil tension strength (1ksf) and the maximum shear strength of the nonlinear soil (23 ksf). Therefore, fracture toughness of 0.001 kip-ft and shear retention factor of 0.002 were assumed in the material model.

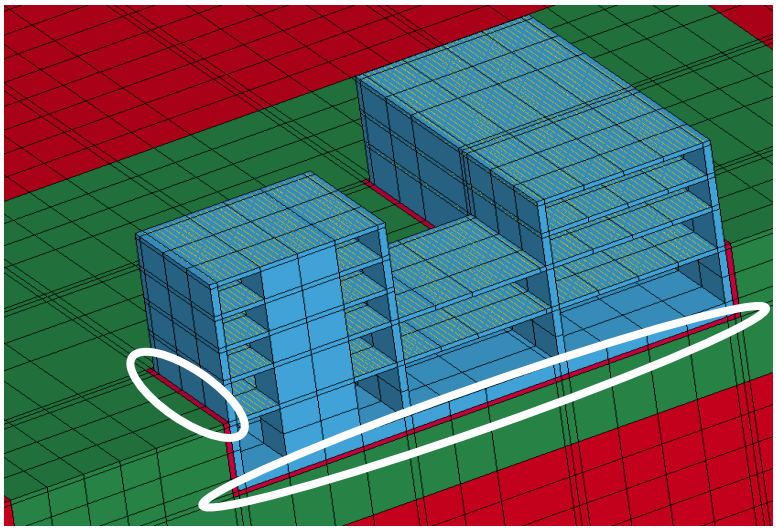

Figure 20. Gap elements in NLSSI-G analysis model.

Figure 21 and Table 9 present the summary of the results from the LSSI-G analysis case. The maximum accelerations at the free field, the bottom of reactor building basemat (RB-BM), and the bottom of turbine building basemat (TB-BM) are compared in the figure and the table. Figure 22 also shows the time history responses at the three locations in three different directions (EW, NS, and UD). As shown in the figures and the table, maximum acceleration values at RB-BM and TB-BM were reduced by 18.0 % in the EW direction, 33.1 % in the NS direction, and 9.2 % in the UD direction. The response spectra converted from the time history responses using the Fast Fourier Transform theorem are shown in Figure 23. The same tendency can be seen from the figure.

Table 8. Results of NLSSI-G analysis case with gap element.

	Maximum Acceleration, g			
Locations	Node Number	EW	NS	UD
Free Field (FF)	377808	0.579	0.428	0.385
Reactor Building Basemat (RB-BM)	648087	0.475	0.297	0.351
Turbine Building Basemat (TB-BM)	648824	0.474	0.276	0.348

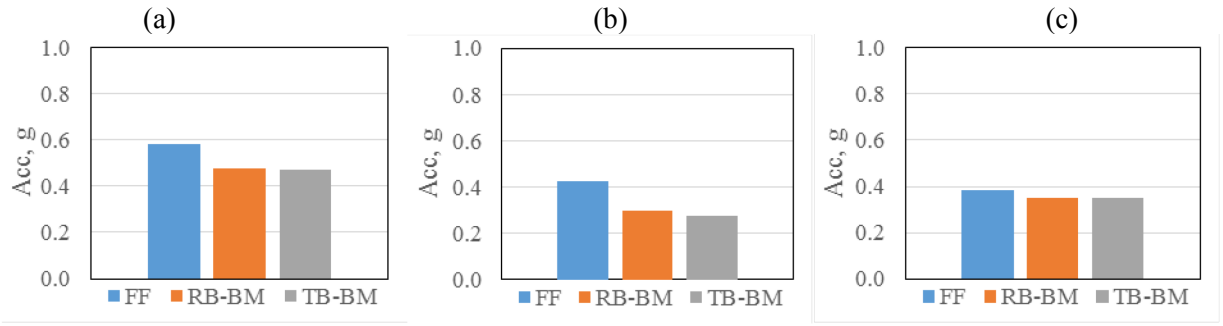

Figure 21. Comparison of maximum acceleration value calculated from NLSSI-G analysis case, Free Field (FF), Reactor Basemat (RB-BM), Turbine Basemat (TB-BM): (a) EW direction, (b) NS direction, and (c) UD direction.

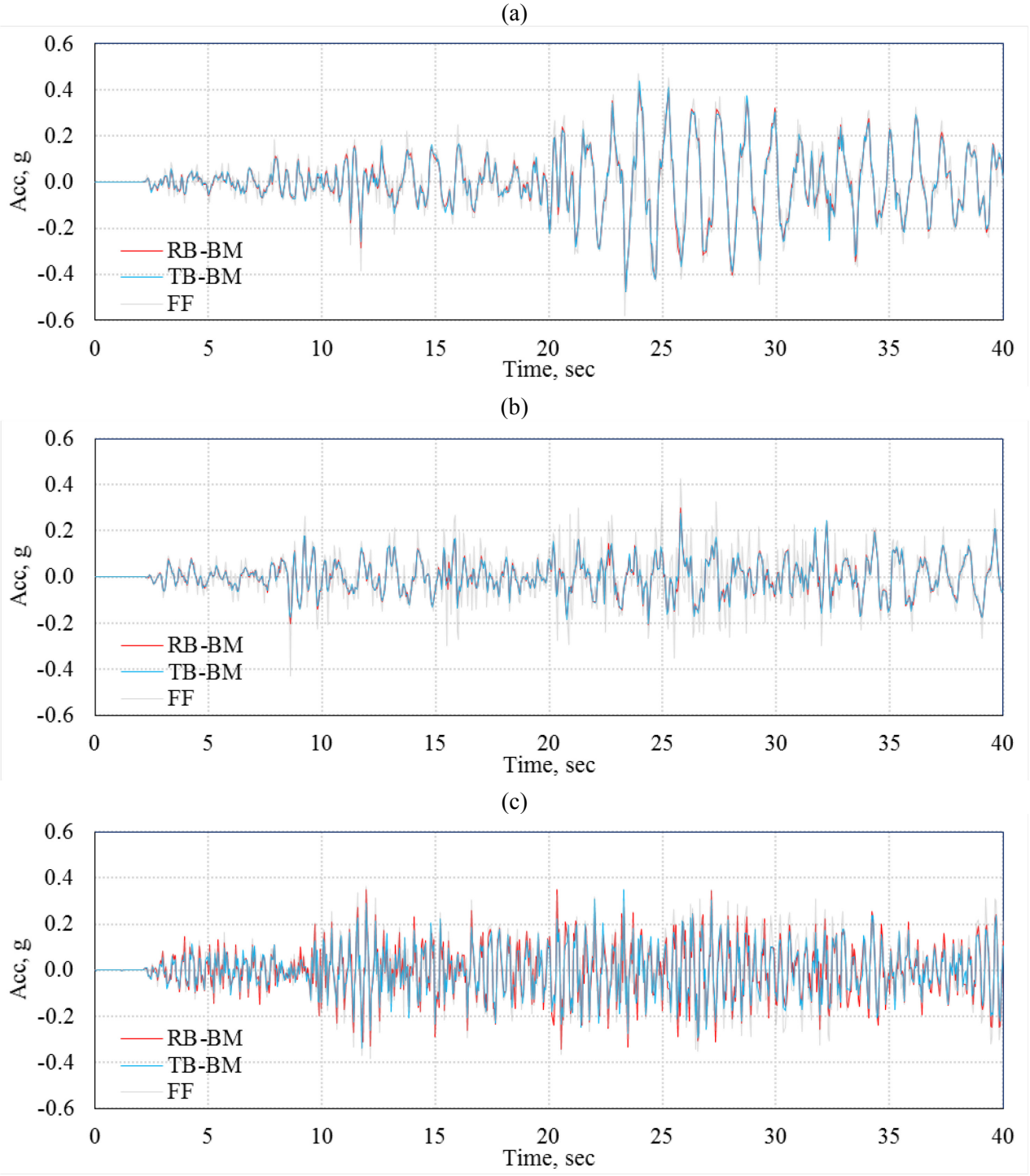

Figure 22. Time history response estimated by LSSI-G analysis case: (a) EW direction, (b) NS direction, and (c) UD direction.

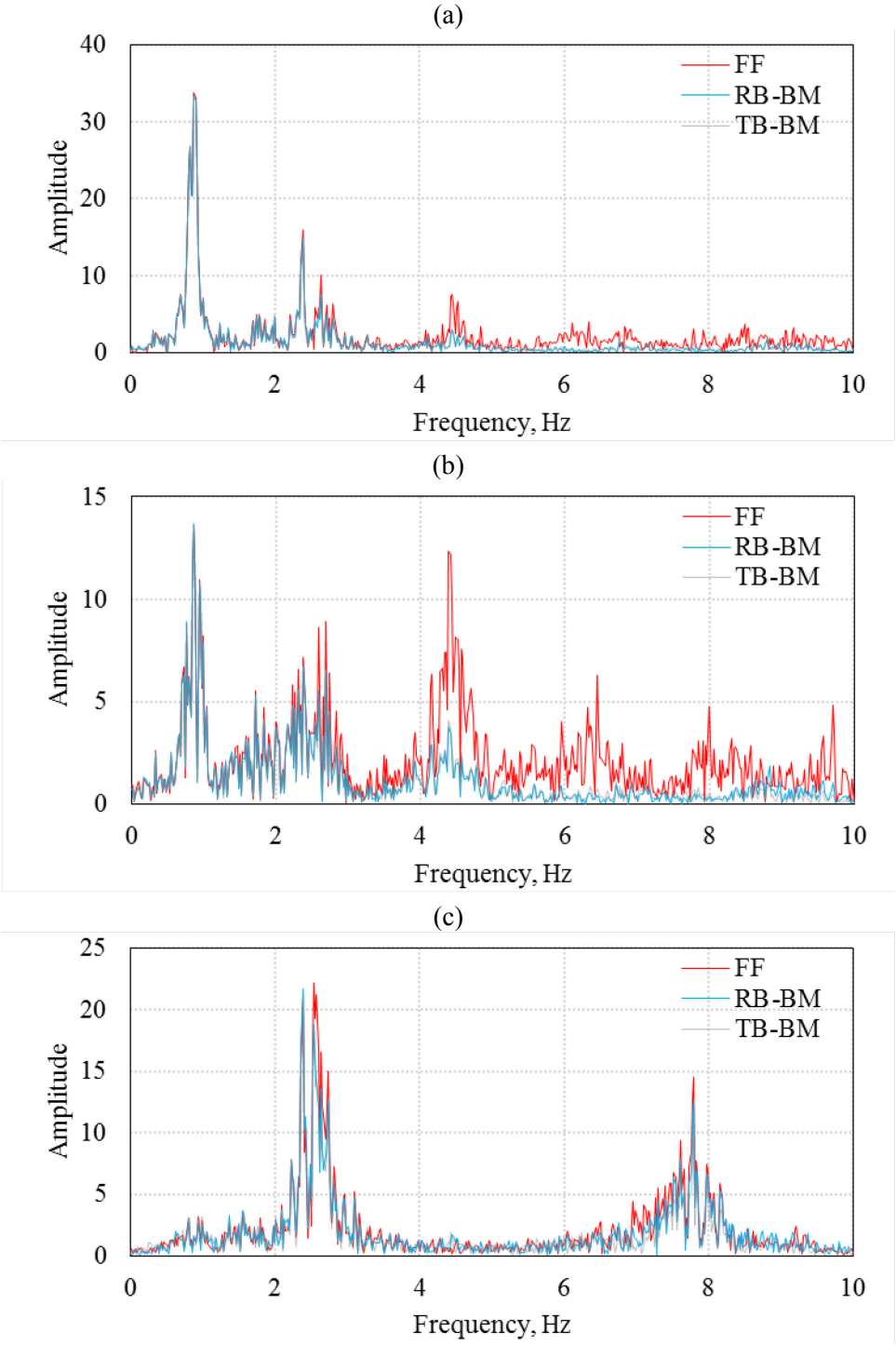

Figure 23. Response spectra of on the free field, RB-BM, and TB-BM converted using the Fast Fourier Transform theorem: (a) EW direction, (b) NS direction, and (c) UD direction.

4. CONCLUSIONS

A series of both linear and nonlinear soil-structure interaction analyses were performed to explore the influence on nonlinearities (material and geometric) on the seismic response (ISRS) of nuclear power plant structures. The study was motivated by the hypothesis that these nonlinearities could potentially reduce the maximum accelerations in the structural basemat relative to the values measured in the free field. Only two sources of nonlinearities were explored in this study: (i) soil material nonlinearity, and (ii) geometric nonlinearity (gapping and sliding) between soil and structure. Linear soil-structure interaction (LSSI) analysis was first performed in the time domain with elastic soil material properties. Nonlinear soil-structure interaction (NLSSI) analyses with nonlinear soil material (NLSSI-S), tiebreak contact definition (NLSSI-TB), and gap elements (NLSSI-G) were also performed.

Maximum accelerations between the free field and basemat were reduced slightly in only the EW and NS directions. The maximum acceleration in the UD direction increased by 10 %. The largest reduction in maximum accelerations occurred in the NLSSI-S model, in which the structure is surrounded by nonlinear soil. Up to 49.8 % of maximum acceleration reduction was observed. The attempt to simulate the geometric nonlinearity (gapping and sliding) using the tiebreak contact in LS-DYNA (NLSSI-TB) resulted in unrealistic amplifications in the structure are due to the reversal to non-automatic contact after failure. The attempt to simulate the geometric nonlinearity (gapping and sliding) using gap elements (NLSSI-G) resulted in similar responses to those as NLSSI-S model. No additional reduction in response was observed due to the nonlinearity at the interface. Therefore, maximum reductions observed in the NLSSI studies documented here were due to the soil nonlinearities. However, this was an exploratory study, which highlights the need for more detailed and focused investigations with due consideration of: (i) the ground motion content (frequency and amplitude), (ii) better modeling of soil nonlinearities, (iii) better modeling of the nonlinearity at the soil-structure interface, and (iv) calibration of the nonlinearity models using experimental data if possible. Experimental calibration of the interface model using direct shear test data is recommended if possible. But, there is a better need to understand this nonlinearity at the soil-concrete interfaces, gapping and sliding elements need to be improved, and sensitivity analysis need to be conducted. Soil tensile strength (range $\pm$ 50 %), interface behavior (range $\pm$ 50%), friction coefficient (range $\pm$ 50%), ground motion PGA (range $\pm$ 25%), soil nonlinearity (variability) should be considered in the sensitivity analysis.

5. REFERENCES

[1] Coleman, J. (2015), “Light Water Reactor Sustainability Program Seismic Data Gathering and Validation,” INL/EXT-15-34425, Idaho National Laboratory, Idaho Falls, Idaho.

[2] Bolisetti, C. and Coleman, J. (2015), “Light Water Reactor Sustainability Program Advanced Seismic Soil Structure Modeling,” INL/EXT-15-35687, Idaho National Laboratory, Idaho Falls, Idaho.

[3] Livermore Software Technology Corporation (LSTC). (2009). "LS-DYNA Theory Manual." Livermore, California.

[4] Livermore Software Technology Corporation (LSTC). (2013). "LS-DYNA Keyword User's Manual - Version R 7.0." Livermore, California.